英文科技论文阅读教程

马新英 林易 任永山 主编

READING ENGLISH SCIENTIFIC PAPERS

国防工业出版社
National Defense Industry Press

英文科技论文阅读教程

Reading English Scientific Papers

主　编　马新英　林　易　任永山

编　者　（按姓氏笔画为序）

马新英　万惠琼　任永山

陈　卓　张娅丽　李艳霞　林　易

国防工业出版社

·北京·

内 容 简 介

本书旨在围绕研究生专业学习和未来工作的实际需求，培养和提高其实际运用英语的能力，即英文专业论文的阅读理解能力。本书按照论文所涉及的专业内容分为电信、计算机、密码学、大地测量、制图学、摄影测量与遥感六部分，每部分包括三篇取自著名国际相关专业期刊的论文，每篇论文后列出了常用专业词汇及涉及阅读理解和关键句型英汉互译的练习，从而强调掌握英文专业论文在用词、造句、文体等方面的风格和特点，并在此基础上阅读理解论文，掌握论文的结构和写法。

本书可作为电信、计算机、密码学、大地测量、制图学、摄影测量与遥感等专业的英语教材，也可作为相关工程技术人员的参考用书。

图书在版编目(CIP)数据

英文科技论文阅读教程／马新英，林易，任永山主编．
—北京：国防工业出版社，2016.6
ISBN 978-7-118-10806-4

Ⅰ.①英… Ⅱ.①马… ②林… ③任… Ⅲ.①英语—科学研究—论文—阅读教学—教材 Ⅳ.①H319.4

中国版本图书馆 CIP 数据核字(2016)第 116980 号

※

国防工业出版社出版发行
（北京市海淀区紫竹院南路 23 号 邮政编码 100048）
三河市鼎鑫印务有限公司印刷
新华书店经售
*
开本 787×1092 1/16 印张 15½ 字数 355 千字
2016 年 6 月第 1 版第 1 次印刷 印数 1—2500 册 定价 38.00 元

国防书店：(010)88540777 发行邮购：(010)88540776
发行传真：(010)88540755 发行业务：(010)88540717

FOREWORD 前言

随着我国高等教育改革的全面深化，研究生公共英语教学也在围绕以学生为中心、以能力培养为导向等现代教育教学理念，从教学内容、模式、方法、手段等方面进一步拓展和深化教学改革。本书的编写就是着眼于更好地服务研究生专业学习和工作的实际需求，培养和提高其实际运用英语的能力。

研究生在学习和未来工作中所面临的一个重要任务就是能高水平地阅读、写作，并发表本专业的英文论文，这的确需要严格的针对性训练。写作是语言的输出，是建立在大量阅读、完成语言输入的基础上的，本书所强调的就是通过大量阅读英文论文掌握论文的基本结构和写法，同时掌握英文专业论文在用词、造句、文体等方面的风格和特点，从而为专业论文写作打下基础。本书按照论文所涉及的专业内容分为电信、计算机、密码学、大地测量、制图学、摄影测量与遥感六部分，每部分包括三篇取自著名国际相关专业期刊的论文，每篇论文后列出了常用专业词汇和涉及阅读理解和关键句型英汉互译的练习。

马新英负责教材的总体设计组织以及第一部分的编写，陈卓编写了第二部分，林易编写了第三部分，张娅丽编写了第四部分，任永山编写了第五部分并完成了全书的统稿工作，万惠琼、李艳霞编写了第六部分。由于水平有限，缺点不足在所难免，敬请批评指正。

编者

2015 年 12 月

CONTENTS 目录

Unit 1 电信 Telecommunications

Paper 1-1 Subscriber Location in CDMA Cellular Networks

James Caffery, Jr., Student Member, IEEE, and Gordon L. Stüber, Senior Member, IEEE

Abstract—Subscriber radio location techniques are investigated for code-division multiple-access (CDMA) cellular networks. Two methods are considered for radio location: measured times of arrival (ToA) and angles of arrival (AoA). The ToA measurements are obtained from the code tracking loop in the CDMA receiver, and the AoA measurements at a base station (BS) are assumed to be made with an antenna array. The performance of the two methods is evaluated for both ranging and two-dimensional (2-D) location, while varying the propagation conditions and the number of BS's used for the location estimate.

Index Terms—Cellular CDMA, position location

I. Introduction

OVER THE past decade, considerable attention has been given to vehicle location technology, and numerous applications have been proposed. Recently, in a few testbed areas, rental cars outfitted with location devices and map displays have aided visitors in unfamiliar territory[1]. Taxi and delivery drivers have utilized location technology in Tokyo to navigate the myriad of streets. Fleet operators use location technology to improve product delivery times and to improve the efficiency of the fleet management process. Emergency and police dispatchers have also utilized location technology to locate dispatch vehicles and emergencies for improved response times. In cellular telephone networks, location technology could be used for radio resource and mobility management [2,3]. For example, a service provider who may have multiple agreements with personal communication services (PCS's), cellular, or satellite carriers, could offer its customers the ability to choose a carrier that best suits their needs at a given time and location[4]. Also, the Federal Communication Commission has recently released an order, to be implemented in two phases, requiring cellular service providers to provide a mechanism for generating subscriber location estimates for Enhanced-911 (E-911) services[5]. A further application of location technology is in the rapidly emerging field of intelligent transportation systems (ITS's), which are designed to enhance highway safety, system operating efficiency, environmental quality, and energy utilization in transportation[6,7]. Each of the above applications requires a method for determining and relaying the location of vehicular and pedestrian mobile stations (MS's).

Automatic vehicle location (AVL) techniques have been studied thoroughly in the literature for the purpose of vehicle location. AVL systems entail the acquisition of information about the location of MS's operating in an area, and all require the processing of that information to form location estimates. There are three basic AVL methods: *dead reckoning*, *proximity systems*, and *radio location* [8]. Dead reckoning computes the direction and distance of travel from a known starting position[8]. In proximity systems, the nearness of an MS to fixed detection devices is used to determine its position. The devices can be anything from magnetic sensors to conventional radio transmitters and receivers.

Radio location systems attempt to locate an MS by measuring the radio signals traveling between the MS and a set of fixed stations (FS's). The signal measurements are first used to determine the length or direction of the radio path, and then the MS position is derived from known geometric relationships[8]. Radio location can be implemented in one of two ways—either the MS transmits a signal which the FS's use to determine its location or the FS's transmit signals that the MS's use to calculate their own positions [e.g., the global positioning system (GPS)]. There are several fundamental approaches for implementing a radio location system including those based on signal-strength[9-12], angle of arrival (AoA)[13], and time of arrival (ToA)[3, 14,15]. It is important to note that line-of-sight (LOS) propagation is necessary for accurate location estimates.

Many of the existing location technologies use dead reckoning, radio location with GPS, or hybrids which require specialized subscriber equipment, the cost of which can severely limit their availability to the average consumer. With these technologies, the MS formulates the location estimate which may be relayed to a central site. Another approach for providing location services is to use the cellular telephone networks. A method has been proposed in [1] which incorporates the cellular network into the location process. However, this service requires a GPS receiver in the MS to determine the location, and the cellular network is only used to relay the location information to a central site. Only one previous work has examined a subscriber location technique that relies solely on the cellular network, which is based on signal attenuation measurements[12].

This paper examines the feasibility and performance of radio location techniques in code-division multiple-access (CDMA) cellular networks. CDMA is the chosen access scheme, since it appears to be the leading candidate for third generation cellular networks. The cellular network is used as the sole means to locate the MS's, and the location estimates are determined through reception of signals that are transmitted by the MS at a set of base stations (BS's). This approach has the advantage of requiring no modifications to the subscriber equipment. Specifically, radio location methods based on AoA and ToA are studied.

The remainder of this paper is organized as follows. Section Ⅱ outlines the methods employed for the AoA and ToA techniques that will be used for the performance evaluation. The propagation models for macrocellular and microcellular systems are discussed in Section Ⅲ, followed by simulation results in Section Ⅳ. A discussion of some practical issues for subscriber

location is given in Section Ⅴ, followed by some concluding remarks in Section Ⅵ.

Ⅱ. Radio Location System

2.1 Angle of Arrival

AoA techniques estimate the location of an MS by using directive antennas or antenna arrays to measure the AoA at several BS's of a signal that is transmitted by the MS[13,16]. Simple geometric relationships are then used to form the location estimate, based on the AoA measurements and the known positions of the BS's. With the AoA method, a position fix requires a minimum of two BS's in a 2-D plane. In this paper, we consider the error due to multipath propagation, but do not consider angle estimation errors. Multipath propagation, in the form of scattering near and around the MS and BS, will affect the measured AoA. For macrocells, scattering objects are primarily within a small distance of the MS since the BS's are usually located well above surrounding objects[17,18]. This results in reception of signals from all directions at an MS while the BS receives signals from a small azimuthal spread. For microcells, it has been suggested that the BS's be placed below rooftop level (lamppost height) in order to confine the signal coverage to a small area [18]. As a result, the BS becomes surrounded by local scatterers and signals can arrive at the BS from a much broader range of angles. Consequently, the AoA approach, which may be used for macrocells, is impractical for microcells.

Gans[14] and Jakes[17] have modeled the macrocellular propagation environment as a ring of scatterers about the MS, with the BS well outside the ring. Fig. 1 illustrates this geometry, where the primary scatterers are assumed to be on a ring of radius a about the MS. The distance between the BS and MS, d, is assumed to be much greater than a. We assume that the MS uses an omnidirectional antenna, so that

$$p(\gamma) = \frac{1}{2\pi}, \quad 0 \leqslant \gamma < 2\pi. \tag{1}$$

The distribution of the AoA at the BS, θ, is given by

$$\frac{\mathrm{d}\gamma}{\mathrm{d}\theta} p(\theta) = 2p(\gamma). \tag{2}$$

From the geometry of Fig. 1, we find that[14]

$$\mathrm{d}\gamma \backsimeq \left[\left(\frac{a}{d}\right)^2 - (\beta - \theta)^2\right]^{-(1/2)} \mathrm{d}\theta. \tag{3}$$

Therefore, $p(\theta)$ is

$$p(\theta) = \begin{cases} K\left[\left(\frac{a}{d}\right)^2 - (\beta - \theta)^2\right]^{-(1/2)}, & \beta - \theta_M \leqslant \theta \leqslant \beta + \theta_M \\ 0, & \text{otherwise} \end{cases} \tag{4}$$

where

$$\theta_M = \arctan(a/d)$$

$$K = \frac{1}{2\arcsin\left(\frac{d\theta_M}{a}\right)}.$$

Note that for $d \gg a$, a small angle approximation can be invoked, with the result that $\theta_M \approx a/d$ and $K \approx 1/\pi$.

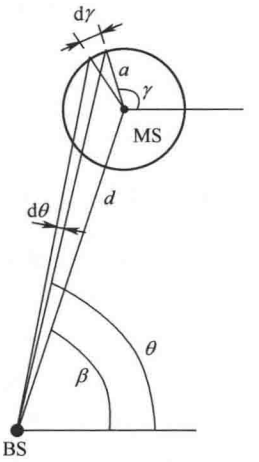

Fig. 1 MS-BS geometry assuming a ring of scatterers for macrocells.

The model $p(\theta)$ provides the AoA distribution for signals arriving at a BS. Our model goes one step further by assuming that a *measured* AoA at a BS also has the distribution $p(\theta)$. Since the measured angles are not equal to the true angles to the MS, the lines of position from the BS's will not intersect at the same point. This problem is resolved by deriving the location estimate from the centroid of the set of points defined by the intersecting lines of position. With three points: (x_1, y_1), (x_2, y_2), and (x_3, y_3). The location estimate $(\hat{x}, \hat{y})$ is obtained by averaging the coordinates of the points of intersection, i.e., $\hat{x} = (x_1 + x_2 + x_3)/3$ and $\hat{y} = (y_1 + y_2 + y_3)/3$.

2.2 Time of Arrival

Many popular radio location techniques are based upon the measurement of the arrival times of a signal transmitted by an MS at several BS's. These methods determine the distance between an MS and BS by measuring the time a signal takes to travel from the BS, to the MS, and back again. Geometrically, this provides a circle, centered at the BS, on which the MS must lie. Using at least three BS's to resolve ambiguities in two dimensions, the intersection of circles provides the MS's position. This method is often called the ToA method and has the disadvantage that it requires the MS to act as a transponder in which processing delays and non-LOS propagation can introduce error. To overcome these limitations, time *difference* measurements rather than absolute time measurements can be used. Since the hyperbola is a curve corresponding to a constant time difference of arrival (TDoA) for two BS's, the time differences define hyperbolas, with foci at the BS's, on which the MS must lie. The intersection of hyperbolas provides the location of the MS. This method is often called the TDoA method. Methods for obtaining the ToA or TDoA estimates include phase ranging[19], pulse ranging[3,19], and spread-spectrum techniques[20, 21].

Since the cellular system being considered is CDMA, methods for determining the ToA's from the spread-spectrum signal are of interest. The two methods for determining time delays in spread-spectrum communications systems are coarse timing acquisition with a sliding correlator or matched filter and fine timing acquisition with a delay-locked loop (DLL) or taudither loop (TDL)[22]. Previous subscriber location studies have used coarse timing acquisition to obtain the ToA estimates[20,21]. Since the DLL finely tracks the time delay, it is better suited for a location system. The DLL is an essential part of time estimation used for GPS and provides

reasonable accuracy over the satellite-earth propagation channel. Here, the DLL-based location system will be investigated for its performance in cellular propagation environments.

The DLL shown in Fig. 2 allows fine synchronization of the local spreading code with the incoming code. It operates by correlating the received signal with the early and late spreading codes $c(t-\hat{\tau}+\Delta T_c)$ and $c(t-\hat{\tau}-\Delta T_c)$, respectively, where $\hat{\tau}$ is an estimate of the delay between the local and incoming codes. The code phase error signal $e(t)$ is obtained by squaring and differencing the correlator outputs. The squaring operations serve to remove the effects of data modulation and carrier phase shift. The loop is closed by applying $e(t)$ to a low-pass filter, whose output is used to drive the voltage-controlled clock (VCC) and correct the code phase error of the locally generated code. The parameter $\Delta, 0<\Delta<1$, is called the *early-late discriminator offset*. The output of the VCC provides the ToA estimate $\hat{\tau}$.

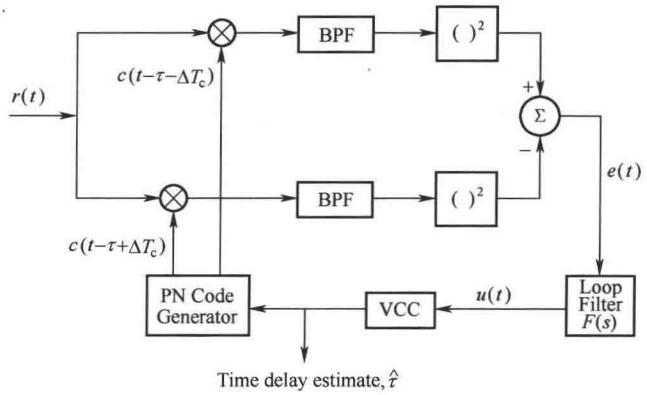

Fig. 2 The DLL used for time-based subscriber location.

2.3 *Time-Based Location Algorithm*

Two approaches are generally used to calculate the location of an MS from ToA or TDoA estimates. One approach uses a geometric interpretation to calculate the intersection of circles or hyperbolas, depending on whether ToA or TDoA is used. This approach becomes difficult if the hyperbolas or circles do not intersect at a point due to time measurement errors. A second approach calculates the position using a nonlinear least-squares (NL-LS) solution[3,19,23], which is a more statistically justifiable approach. The algorithm assumes that the MS, located at (x_0, y_0), transmits its sequence at time τ_0. The N BS receivers located at coordinates (x_1, y_1), (x_2, y_2), $\cdots$, and (x_N, y_N) receive the sequence at times $\tau_1, \tau_2, \cdots, \tau_N$. As a performance measure, we consider the function[19]

$$f_i(x) = c(\tau_i - \tau) - \sqrt{(x_i - x)^2 + (y_i - y)^2} \tag{5}$$

where c is the speed of light, and $x=(x, y, \tau)^T$. This function is formed for each BS receiver, $i=1, \cdots, N$, and all the $f_i(x)$ could be made zero with the proper choice of x, y, and τ. However, the measured values of the arrival times τ_i are generally in error due to multipath and other impairments, and non-LOS propagation introduces errors into the range estimates that are derived from the arrival times.

1) *Unconstrained NL-LS Approach*: To obtain the location estimate from the raw ToA data,

the following function is formed:

$$F(x) = \sum_{i=1}^{N} \alpha_i^2 f_i^2(x) \tag{6}$$

where the a_i's are weights reflecting the reliability of the signal received at BS i. The location estimate is determined by minimizing the function $F(x)$.

A simple approach for solving the nonlinear least squares problem in (6) is the steepest descent method, where successive location estimates are updated according to the recursion

$$x_{k+1} = x_k - \mu \nabla_x F(x_k) \tag{7}$$

where μ is a constant(scalar or diagonal matrix), $x_k = (x_k, y_k, \tau_k)^{\mathrm{T}}$, $\nabla_x \equiv \mathrm{d}/\mathrm{d}x$, and

$$\nabla_x F(x_k) \equiv \nabla_x F(x) \mid_{x_k} = \begin{pmatrix} \left.\dfrac{\delta F}{\delta x}\right|_{x_k} \\ \left.\dfrac{\delta F}{\delta y}\right|_{y_k} \\ \left.\dfrac{\delta F}{\delta \tau}\right|_{\tau_k} \end{pmatrix} \tag{8}$$

$$= \begin{bmatrix} 2\sum_{i=1}^{N} \alpha_i^2 f_i(x_k) \dfrac{x_i - x_k}{\sqrt{(x_i - x_k)^2 + (y_i - y_k)^2}} \\ 2\sum_{i=1}^{N} \alpha_i^2 f_i(x_k) \dfrac{y_i - y_k}{\sqrt{(x_i - x_k)^2 + (y_i - y_k)^2}} \\ -2c\sum_{i=1}^{N} f_i(x_k) \end{bmatrix} \tag{9}$$

Since τ is small (microseconds) compared to x and y (meters), the scalar step size μ should be small enough to allow τ to converge to a solution. Consequently, μ is chosen to be the diagonal matrix

$$\mu = \begin{bmatrix} \mu_x & 0 & 0 \\ 0 & \mu_y & 0 \\ 0 & 0 & \mu_\tau \end{bmatrix} \tag{10}$$

where $\mu_x, \mu_y \gg \mu_\tau$. The recursion in (7) continues until $\| \nabla_x F(x_k) \|$ is smaller than some prescribed tolerance ε.

One drawback of the steepest descent method is its slow convergence. Other algorithms have been investigated[19,23], which form the solution to (6) by linearizing $f_i(x)$ with a Taylor series expansion about x_k and keeping only the first order terms, i.e.,

$$f_i(x) \approx f_i(x_k) + \delta^{\mathrm{T}} \nabla_x f_i(x_k) \tag{11}$$

where $\delta = (\delta_x, \delta_y, \delta_\tau)^{\mathrm{T}} = x - x_k$. Substituting (11) into (6) and solving

$$\nabla_\delta F(x) = 0 \tag{12}$$

for δ, the vector x_k is updated by

$$x_{k+1} = x_k + \delta. \tag{13}$$

This new estimate is substituted back into (11) and the process is reiterated until $|\delta_x| + |\delta_y| + c|\delta_\tau| < \varepsilon$, where ε is a prescribed tolerance.

When the MS is either close to the BS's or near the perimeter of the area defined by the polygon with the BS's as its vertices, then the linear approximation approach has convergence problems[3,19]. For microcells, the MS is always within a short distance of the serving BS, so this method is not appropriate. The convergence problem arises from the approximation of $f_i(x)$ with the linear terms of the Taylor series expansion. Other objective functions $F(x)$ can be formed replacing, for example, $f_i^2(x)$ with $|f_i(x)|$. However, these methods usually do not perform as well as minimizing the sum of squares[3].

2) *Constrained NL-LS Approach*: It may be possible to improve the time-based location algorithm due to the fact that the range error is always positive[24]. This is because the ToA estimates are always greater than the true ToA values due to multipath propagation and other impairments. Also, the range estimates derived from the ToA estimates are greater than the true ranges due to non-LOS propagation. Therefore, the true location of the MS must lie inside the circles of radius $r_i = c(\tau_i - \tau)$, $i = 1, \cdots, N$, about the BS's, since the MS cannot lie farther from a BS than its corresponding range estimate (Fig. 3). Mathematically, this implies

$$r_i = c(\tau_i - \tau) \geqslant \sqrt{(x_i - x)^2 + (y_i - y)^2} \tag{14}$$

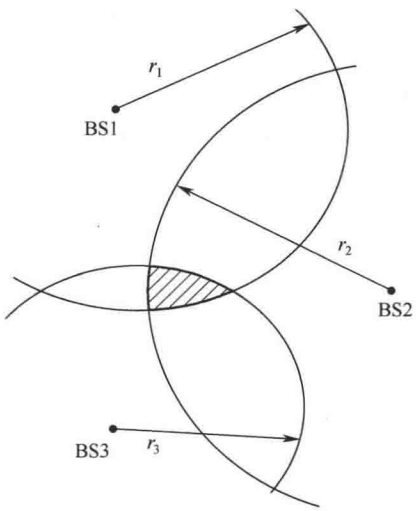

Fig. 3 The location of the MS is constrained to the intersection area (shaded region) of circles of radius $c(\tau_i - \tau)$ centered at each BS.

where (x, y) is the position of the MS. Since the unconstrained NL-LS algorithm does not take this restriction into account, a constrained NL-LS approach can be used to force the estimate at each iteration to satisfy (14). However, the LS solution is complicated by the nonlinear functionals $f_i(x)$ as well as the nonlinear inequality constraints of (14). Note that (14) implies that

$$\sqrt{(x_i - x)^2 + (y_i - y)^2} - c(\tau_i - \tau) \leqslant 0. \tag{15}$$

We recognize from (5) that the left side of the inequality in (15) is simply $g_i(x) = -f_i(x)$. Hence, the restrictions $f_i(x) \geqslant 0$ are formed, where the area within the constraint boundaries is known as the *feasible region.*

There are many approaches to forming numerical solutions for NL-LS problems with nonlinear inequality constraints of the form $g_i(x) \leqslant 0$[25]. One simple, yet effective, method uses penalty functions to modify the objective function $F(x)$ and form a solution using an unconstrained approach as in the previous section. The penalty functions provide a large penalty to the objective function when one or more of the constraints are violated. The objective function in (6) is modified to include the penalty functions $g_i(x)$ as follows[25]:

$$F(x) = \sum_{i=1}^{N} \alpha_i^2 f_i^2(x) - P \sum_{i=1}^{N} [g_i(x)]^{-1} \tag{16}$$

where P is positive for minimization. As any constraint is approached during the search, the penalty term forces F toward infinity, thus forming a natural optimum within the feasible region. This approach requires that the initial guess be placed within the feasible region. A method for doing this is described in[25].

The search procedure can be viewed as the optimization of a sequence of surfaces which tend toward the true value of the objective function. Initially, an unconstrained search method is used to provide an artificial optimum x_1 with a large value of $P = P_1$. The next stage is initialized with the previous estimate x_1 and uses a smaller $P = P_2$ to provide a better approximation to the true optimum. In this way, the solution approaches the constraints more closely, if the optimum happens to lie close to one of the constraints. The penalty constraints become smaller at each stage, forming a monotonic-decreasing sequence $P_1 > P_2 > \cdots$, and the sequence of artificial optima $x_1, x_2, \cdots$tends toward the true optimum. The search continues until several iterations fail to produce a change in the objective function. This formulation essentially replaces a constrained optimization by a sequence of unconstrained optimizations.

Ⅲ. Propagation Models

A three-stage model is used for the radio propagation environment, that includes multipath-fading, shadowing, and path loss. The particular models used in this paper for macrocellular and microcellular propagation environments are now described.

3.1 Macrocells

For wideband spread-spectrum systems, the channel can be modeled by the M-tap tapped delay line

$$h(t) = \sum_{i=0}^{M} w_i(t) \delta(t - \tau_i) \tag{17}$$

where the $\{\tau_i\}$ are the tap delays and the $\{w_i\}$ are the tap gains, assumed here to be complex Gaussian random processes. For numerical convenience, the tap delays can be chosen to be an integer multiple of some small delay τ, i.e., $\tau_i = k_i \tau, i = 1, \ldots, M$. The first tap delay τ_0 is

determined from the MS-BS geometry of Fig. 1 by calculating the distance traveled by a signal transmitted from the MS in a random direction according to $p(\gamma)$ and reflected from the ring of scatterers to the BS. The remaining delays are chosen according to the six-tap reduced typical urban delay profile defined in COST207[26] (see Table 1). The model deviates slightly from the COST 207 Model by assuming a classical Doppler spectrum for all taps, i.e., in the simulations the taps gains are all generated by using Jakes' method[17].

Shadow fades have been described from measurements as being lognormally distributed with a standard deviation that depends on the frequency and the environment[18]. Gudmundson[27] has suggested a simple Markovian model to describe variations in the local mean envelope (or squared envelope) level due to shadow variations. With this model

$$\Omega_{k+1(\mathrm{dB})} = \xi\Omega_{k(\mathrm{dB})} + (1-\xi)_{\eta_k} \qquad (18)$$

Table 1

COST207 S_{IX}-T_{AP} REDUCED TYPICAL URBAN POWER DELAY PROFILE

COST 207 Model	
Delay-τ_0(μs)	Fractional Power
0.0	0.189
0.2	0.379
0.5	0.239
1.6	0.095
2.3	0.061
5.0	0.037

where Ω_k(dB) is the local mean envelope (or square envelope) level (in decibels) that is experienced at location, k, ξ is a parameter that controls the spatial decorrelation of the shadowing, and $\{\eta_k\}$ is a zero-mean discrete-time Gaussian random process with autocorrelation $\phi_{\eta\eta(n)} = \widetilde{\sigma}^2\delta(n)$. The autocorrelation of $\Omega_{k(\mathrm{dB})}$ is given by

$$\phi_{\Omega_{(\mathrm{dB})}\Omega_{(\mathrm{dB})}}(n) = \frac{1-\xi}{1+\xi}\widetilde{\sigma}^2\xi^{|n|} = \sigma_s^2\xi^{|n|} \qquad (19)$$

where o_s is called the shadow standard deviation. Typical values of the shadow standard deviation range from 5 to 12 dB in macrocells[17,18,28]. If we assume that the local mean is sampled every T s, then the autocorrelation can be expressed as

$$\phi_{\Omega_{(\mathrm{dB})}\Omega_{(\mathrm{dB})}}(k) \equiv \phi_{\Omega_{(\mathrm{dB})}\Omega_{(\mathrm{dB})}}(n = kT) = \sigma_s^2 \in_D^{(vT/D)|k|} \qquad (20)$$

where ε_D determines the correlation between two points separated by a spatial distance D and v is the velocity of the MS. The simulations in the sequel assume a shadow decorrelation of 0.1 at a distance of 30 m.

Several empirical path loss models have been presented in the literature, one of the most useful being Hata's model[28], which expresses the path loss in terms of the carrier frequency, BS height, MS antenna height, and the type of environment (urban, suburban, or rural). Hata's model for medium or small city urban areas is used in the sequel with a carrier frequency of f=850 MHz, BS antenna height of 100 m, and an MS antenna height of 2.5 m.

3.2 Microcells

The wideband channel and shadowing models discussed above can also be used to model microcellular propagation. However, the power delay profiles are different, and the standard deviation of shadowing in microcells typically ranges from 4 to 13 dB. Further differences in the

propagation models for microcells and macrocells are discussed in the following.

Microcellular path loss is often described by a two-slope characteristic, where the area mean $\overline{\Omega}=E|\Omega|$ is given by[29]

$$\overline{\Omega} = 10\lg\left[\frac{A}{d^a(1 + d/g)^b}\right] \text{ dBm} \tag{21}$$

where A is a constant, d is the radio path length, g is the break point (that ranges from 150 to 300m), and a and b determine the slopes before and after the break point. In the simulations, we assume $g=150$ m and $a=b=2$.

An important consideration for microcells is the *corner effect*, which occurs in microcellular scenarios when an MS rounds a street corner. To account for this effect, LOS propagation is assumed to the MS until it rounds the corner. The non-LOS propagation after rounding a street corner is modeled by assuming LOS propagation from an imaginary transmitter that is located at the street corner having a transmit power equal to the received power at the street corner from the serving BS. The area mean (in dBm) is given by (22), at the bottom of the next page, where d_c is the distance between the serving BS and the corner.

Due to the site-specific nature of the microcellular propagation environment, techniques such as ray tracing have been developed. In this study, ray tracing concepts are used to calculate the propagation delays for the wideband channel model. A Manhattan street microcell BS deployment is assumed as shown in Fig. 4. When the MS is LOS with a BS, a four-path model is used, consisting of a direct path, a road-reflected path, and two wall-reflected paths. The taps of the wideband channel model are generated using Jakes' method, appropriately modified for Rician fading. When the MS is non-LOS with a BS, i.e., around the corner, a different approach is taken to determine the propagation delays. Since the literature provides no results that describe the power delay profile for an MS that is around a corner from a BS, a simplistic model is chosen. A four-path non-LOS propagation model is used that includes two paths that arrive from diffractions at the building corners in the street intersection and two remaining paths whose delays are generated by adding random delays to the first two paths. All paths are assumed to be Rayleigh faded. The model chosen here is inconsequential, because the extra time delay for non-LOS BS's introduces a large amount of error into the location algorithm. Hence, accurate modeling of multipath propagation on non-LOS streets is not necessary; only a means of introducing the excess propagation delay around the street corner is needed.

Ⅳ. Simulations

The location techniques described in Section II were simulated in the macrocellular and microcellular environments described in Section III to determine their performance. The spreading code used was an m sequence of length 127 and chip rate $T_c^{-1}=1.2288$ Mcps. In the DLL, an all-pass filter

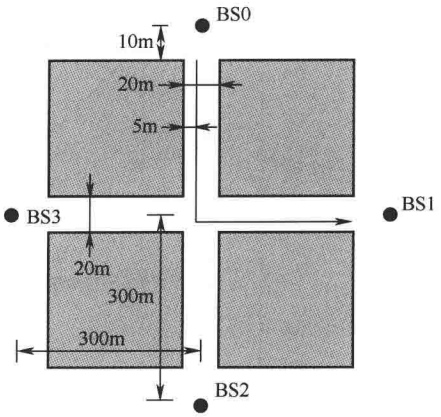

Fig. 4 Manhattan street microcell deployment.

$$\overline{\Omega} \sim \begin{cases} 10\lg\left[\dfrac{1}{d^a(1+d/g)^b}\right], & d \leqslant d_c \\ \lg\left\{\dfrac{1}{d_c^a(1+d_c/g)^b}\cdot\dfrac{1}{(d-d_c)^a[1+(d-d_c)/g]^b}\right\}, & d > d_c \end{cases} \tag{22}$$

was used for the loop filter [i.e., $F(s)=1$]. For the VCC, the output time delay estimate and input waveform are related by

$$\hat{\tau}(t) = K_{\mathrm{VCC}} T_c \int_0^t u(x)\,\mathrm{d}x \tag{23}$$

where K_{VCC} is the gain of the VCC, T_c is the chip period, $u(t)$ is the output of the loop filter, and the VCC is assumed to begin operating at time $t=0$. A simple accumulator models the operation of the VCC in the computer simulations with the constant $K_{\mathrm{VCC}} T_c = 0.003$. Note that there is a limitation in the accuracy that can be achieved when simulating the DLL on a computer. As a result, we limit the resolution of the DLL to 1/120 of a chip to limit the simulation time. Consequently, the ranging resolution is limited to approximately 2 m, which causes all range estimates to be in error even in the absence of propagation impairments. However, with such a fine resolution, propagation impairments will be the predominant source of location error.

4.1 Range Estimation

Ranging measures the 1-D distance between an MS and BS. Only the time-based method is employed for ranging since AoA ranging does not make sense. For macrocells, our ranging results assume that the first path to arrive from the COST 207 model is a LOS path. Consequently, the ranging results for macrocells are very optimistic by disregarding the extra propagation caused by non-LOS propagation when a direct path does not exist. For microcells, the Manhattan street microcell deployment in Fig. 4 is assumed.

1) *Effect of Standard Deviation of Shadowing*, σ_s: Fig. 5(a) shows the effect of the shadow standard deviation on the mean and standard deviation of the range estimation error with an